Measurement of the top quark mass with dilepton events selected using neuroevolution at CDF

T. Aaltonen,[24] J. Adelman,[14] T. Akimoto,[56] M.G. Albrow,[18] B. Álvarez González,[12] S. Amerio[u],[44] D. Amidei,[35] A. Anastassov,[39] A. Annovi,[20] J. Antos,[15] G. Apollinari,[18] A. Apresyan,[49] T. Arisawa,[58] A. Artikov,[16] W. Ashmanskas,[18] A. Attal,[4] A. Aurisano,[54] F. Azfar,[43] P. Azzurri[s],[47] W. Badgett,[18] A. Barbaro-Galtieri,[29] V.E. Barnes,[49] B.A. Barnett,[26] V. Bartsch,[31] G. Bauer,[33] P.-H. Beauchemin,[34] F. Bedeschi,[47] P. Bednar,[15] D. Beecher,[31] S. Behari,[26] G. Bellettini[q],[47] J. Bellinger,[60] D. Benjamin,[17] A. Beretvas,[18] J. Beringer,[29] A. Bhatti,[51] M. Binkley,[18] D. Bisello[u],[44] I. Bizjak,[31] R.E. Blair,[2] C. Blocker,[7] B. Blumenfeld,[26] A. Bocci,[17] A. Bodek,[50] V. Boisvert,[50] G. Bolla,[49] D. Bortoletto,[49] J. Boudreau,[48] A. Boveia,[11] B. Brau,[11] A. Bridgeman,[25] L. Brigliadori,[44] C. Bromberg,[36] E. Brubaker,[14] J. Budagov,[16] H.S. Budd,[50] S. Budd,[25] K. Burkett,[18] G. Busetto[u],[44] P. Bussey[x],[22] A. Buzatu,[34] K. L. Byrum,[2] S. Cabrera[p],[17] C. Calancha,[32] M. Campanelli,[36] M. Campbell,[35] F. Canelli,[18] A. Canepa,[46] D. Carlsmith,[60] R. Carosi,[47] S. Carrillo[j],[19] S. Carron,[34] B. Casal,[12] M. Casarsa,[18] A. Castro[t],[6] P. Catastini[r],[47] D. Cauz[w],[55] V. Cavaliere[r],[47] M. Cavalli-Sforza,[4] A. Cerri,[29] L. Cerrito[n],[31] S.H. Chang,[28] Y.C. Chen,[1] M. Chertok,[8] G. Chiarelli,[47] G. Chlachidze,[18] F. Chlebana,[18] K. Cho,[28] D. Chokheli,[16] J.P. Chou,[23] G. Choudalakis,[33] S.H. Chuang,[53] K. Chung,[13] W.H. Chung,[60] Y.S. Chung,[50] C.I. Ciobanu,[45] M.A. Ciocci[r],[47] A. Clark,[21] D. Clark,[7] G. Compostella,[44] M.E. Convery,[18] J. Conway,[8] K. Copic,[35] M. Cordelli,[20] G. Cortiana[u],[44] D.J. Cox,[8] F. Crescioli[q],[47] C. Cuenca Almenar[p],[8] J. Cuevas[m],[12] R. Culbertson,[18] J.C. Cully,[35] D. Dagenhart,[18] M. Datta,[18] T. Davies,[22] P. de Barbaro,[50] S. De Cecco,[52] A. Deisher,[29] G. De Lorenzo,[4] M. Dell'Orso[q],[47] C. Deluca,[4] L. Demortier,[51] J. Deng,[17] M. Deninno,[6] P.F. Derwent,[18] G.P. di Giovanni,[45] C. Dionisi[v],[52] B. Di Ruzza[w],[55] J.R. Dittmann,[5] M. D'Onofrio,[4] S. Donati[q],[47] P. Dong,[9] J. Donini,[44] T. Dorigo,[44] S. Dube,[53] J. Efron,[40] A. Elagin,[54] R. Erbacher,[8] D. Errede,[25] S. Errede,[25] R. Eusebi,[18] H.C. Fang,[29] S. Farrington,[43] W.T. Fedorko,[14] R.G. Feild,[61] M. Feindt,[27] J.P. Fernandez,[32] C. Ferrazza[s],[47] R. Field,[19] G. Flanagan,[49] R. Forrest,[8] M. Franklin,[23] J.C. Freeman,[18] I. Furic,[19] M. Gallinaro,[52] J. Galyardt,[13] F. Garberson,[11] J.E. Garcia,[47] A.F. Garfinkel,[49] K. Genser,[18] H. Gerberich,[25] D. Gerdes,[35] A. Gessler,[27] S. Giagu[v],[52] V. Giakoumopoulou,[3] P. Giannetti,[47] K. Gibson,[48] J.L. Gimmell,[50] C.M. Ginsburg,[18] N. Giokaris,[3] M. Giordani[w],[55] P. Giromini,[20] M. Giunta[q],[47] G. Giurgiu,[26] V. Glagolev,[16] D. Glenzinski,[18] M. Gold,[38] N. Goldschmidt,[19] A. Golossanov,[18] G. Gomez,[12] G. Gomez-Ceballos,[33] M. Goncharov,[54] O. González,[32] I. Gorelov,[38] A.T. Goshaw,[17] K. Goulianos,[51] A. Gresele[u],[44] S. Grinstein,[23] C. Grosso-Pilcher,[14] R.C. Group,[18] U. Grundler,[25] J. Guimaraes da Costa,[23] Z. Gunay-Unalan,[36] C. Haber,[29] K. Hahn,[33] S.R. Hahn,[18] E. Halkiadakis,[53] B.-Y. Han,[50] J.Y. Han,[50] R. Handler,[60] F. Happacher,[20] K. Hara,[56] D. Hare,[53] M. Hare,[57] S. Harper,[43] R.F. Harr,[59] R.M. Harris,[18] M. Hartz,[48] K. Hatakeyama,[51] J. Hauser,[9] C. Hays,[43] M. Heck,[27] A. Heijboer,[46] B. Heinemann,[29] J. Heinrich,[46] C. Henderson,[33] M. Herndon,[60] J. Heuser,[27] S. Hewamanage,[5] D. Hidas,[17] C.S. Hill[c],[11] D. Hirschbuehl,[27] A. Hocker,[18] S. Hou,[1] M. Houlden,[30] S.-C. Hsu,[10] B.T. Huffman,[43] R.E. Hughes,[40] U. Husemann,[61] J. Huston,[36] J. Incandela,[11] G. Introzzi,[47] M. Iori[v],[52] A. Ivanov,[8] E. James,[18] B. Jayatilaka,[17] E.J. Jeon,[28] M.K. Jha,[6] S. Jindariani,[18] W. Johnson,[8] M. Jones,[49] K.K. Joo,[28] S.Y. Jun,[13] J.E. Jung,[28] T.R. Junk,[18] T. Kamon,[54] D. Kar,[19] P.E. Karchin,[59] Y. Kato,[42] R. Kephart,[18] J. Keung,[46] V. Khotilovich,[54] B. Kilminster,[40] D.H. Kim,[28] H.S. Kim,[28] J.E. Kim,[28] M.J. Kim,[20] S.B. Kim,[28] S.H. Kim,[56] Y.K. Kim,[14] N. Kimura,[56] L. Kirsch,[7] S. Klimenko,[19] B. Knuteson,[33] B.R. Ko,[17] S.A. Koay,[11] K. Kondo,[58] D.J. Kong,[28] J. Konigsberg,[19] A. Korytov,[19] A.V. Kotwal,[17] M. Kreps,[27] J. Kroll,[46] D. Krop,[14] N. Krumnack,[5] M. Kruse,[17] V. Krutelyov,[11] T. Kubo,[56] T. Kuhr,[27] N.P. Kulkarni,[59] M. Kurata,[56] Y. Kusakabe,[58] S. Kwang,[14] A.T. Laasanen,[49] S. Lami,[47] S. Lammel,[18] M. Lancaster,[31] R.L. Lander,[8] K. Lannon,[40] A. Lath,[53] G. Latino[r],[47] I. Lazzizzera[u],[44] T. LeCompte,[2] E. Lee,[54] S.W. Lee[o],[54] S. Leone,[47] J.D. Lewis,[18] C.S. Lin,[29] J. Linacre,[43] M. Lindgren,[18] E. Lipeles,[10] A. Lister,[8] D.O. Litvintsev,[18] C. Liu,[48] T. Liu,[18] N.S. Lockyer,[46] A. Loginov,[61] M. Loreti[u],[44] L. Lovas,[15] R.-S. Lu,[1] D. Lucchesi[u],[44] J. Lueck,[27] C. Luci[v],[52] P. Lujan,[29] P. Lukens,[18] G. Lungu,[51] L. Lyons,[43] J. Lys,[29] R. Lysak,[15] E. Lytken,[49] P. Mack,[27] D. MacQueen,[34] R. Madrak,[18] K. Maeshima,[18] K. Makhoul,[33] T. Maki,[24] P. Maksimovic,[26] S. Malde,[43] S. Malik,[31] G. Manca[y],[30] A. Manousakis-Katsikakis,[3] F. Margaroli,[49] C. Marino,[27] C.P. Marino,[25] A. Martin,[61] V. Martin[i],[22] M. Martínez,[4] R. Martínez-Ballarín,[32] T. Maruyama,[56] P. Mastrandrea,[52] T. Masubuchi,[56] M.E. Mattson,[59] P. Mazzanti,[6] K.S. McFarland,[50] P. McIntyre,[54] R. McNulty[h],[30] A. Mehta,[30] P. Mehtala,[24] A. Menzione,[47] P. Merkel,[49] C. Mesropian,[51] T. Miao,[18] N. Miladinovic,[7] R. Miller,[36] C. Mills,[23] M. Milnik,[27] A. Mitra,[1] G. Mitselmakher,[19] H. Miyake,[56] N. Moggi,[6] C.S. Moon,[28] R. Moore,[18] M.J. Morello[q],[47] J. Morlok,[27] P. Movilla Fernandez,[18]

J. Mülmenstädt,[29] A. Mukherjee,[18] Th. Muller,[27] R. Mumford,[26] P. Murat,[18] M. Mussini[t],[6] J. Nachtman,[18] Y. Nagai,[56] A. Nagano,[56] J. Naganoma,[58] K. Nakamura,[56] I. Nakano,[41] A. Napier,[57] V. Necula,[17] C. Neu,[46] M.S. Neubauer,[25] J. Nielsen[e],[29] L. Nodulman,[2] M. Norman,[10] O. Norniella,[25] E. Nurse,[31] L. Oakes,[43] S.H. Oh,[17] Y.D. Oh,[28] I. Oksuzian,[19] T. Okusawa,[42] R. Orava,[24] K. Osterberg,[24] S. Pagan Griso[u],[44] C. Pagliarone,[47] E. Palencia,[18] V. Papadimitriou,[18] A. Papaikonomou,[27] A.A. Paramonov,[14] B. Parks,[40] S. Pashapour,[34] J. Patrick,[18] G. Pauletta[w],[55] M. Paulini,[13] C. Paus,[33] D.E. Pellett,[8] A. Penzo,[55] T.J. Phillips,[17] G. Piacentino,[47] E. Pianori,[46] L. Pinera,[19] K. Pitts,[25] C. Plager,[9] L. Pondrom,[60] O. Poukhov[*],[16] N. Pounder,[43] F. Prakoshyn,[16] A. Pronko,[18] J. Proudfoot,[2] F. Ptohos[g],[18] E. Pueschel,[13] G. Punzi[q],[47] J. Pursley,[60] J. Rademacker[c],[43] A. Rahaman,[48] V. Ramakrishnan,[60] N. Ranjan,[49] I. Redondo,[32] B. Reisert,[18] V. Rekovic,[38] P. Renton,[43] M. Rescigno,[52] S. Richter,[27] F. Rimondi[t],[6] L. Ristori,[47] A. Robson,[22] T. Rodrigo,[12] T. Rodriguez,[46] E. Rogers,[25] S. Rolli,[57] R. Roser,[18] M. Rossi,[55] R. Rossin,[11] P. Roy,[34] A. Ruiz,[12] J. Russ,[13] V. Rusu,[18] H. Saarikko,[24] A. Safonov,[54] W.K. Sakumoto,[50] O. Saltó,[4] L. Santi[w],[55] S. Sarkar[v],[52] L. Sartori,[47] K. Sato,[18] A. Savoy-Navarro,[45] T. Scheidle,[27] P. Schlabach,[18] A. Schmidt,[27] E.E. Schmidt,[18] M.A. Schmidt,[14] M.P. Schmidt[†],[61] M. Schmitt,[39] T. Schwarz,[8] L. Scodellaro,[12] A.L. Scott,[11] A. Scribano[r],[47] F. Scuri,[47] A. Sedov,[49] S. Seidel,[38] Y. Seiya,[42] A. Semenov,[16] L. Sexton-Kennedy,[18] A. Sfyrla,[21] S.Z. Shalhout,[59] T. Shears,[30] R. Shekhar,[17] P.F. Shepard,[48] D. Sherman,[23] M. Shimojima[l],[56] S. Shiraishi,[14] M. Shochet,[14] Y. Shon,[60] I. Shreyber,[37] A. Sidoti,[47] P. Sinervo,[34] A. Sisakyan,[16] A.J. Slaughter,[18] J. Slaunwhite,[40] K. Sliwa,[57] J.R. Smith,[8] F.D. Snider,[18] R. Snihur,[34] A. Soha,[8] S. Somalwar,[53] V. Sorin,[36] J. Spalding,[18] T. Spreitzer,[34] P. Squillacioti[r],[47] M. Stanitzki,[61] R. St. Denis,[22] B. Stelzer,[9] O. Stelzer-Chilton,[43] D. Stentz,[39] J. Strologas,[38] D. Stuart,[11] J.S. Suh,[28] A. Sukhanov,[19] I. Suslov,[16] T. Suzuki,[56] A. Taffard[d],[25] R. Takashima,[41] Y. Takeuchi,[56] R. Tanaka,[41] M. Tecchio,[35] P.K. Teng,[1] K. Terashi,[51] J. Thom[f],[18] A.S. Thompson,[22] G.A. Thompson,[25] E. Thomson,[46] P. Tipton,[61] V. Tiwari,[13] S. Tkaczyk,[18] D. Toback,[54] S. Tokar,[15] K. Tollefson,[36] T. Tomura,[56] D. Tonelli,[18] S. Torre,[20] D. Torretta,[18] P. Totaro[w],[55] S. Tourneur,[45] Y. Tu,[46] N. Turini[r],[47] F. Ukegawa,[56] S. Vallecorsa,[21] N. van Remortel[a],[24] A. Varganov,[35] E. Vataga[s],[47] F. Vázquez[j],[19] G. Velev,[18] C. Vellidis,[3] V. Veszpremi,[49] M. Vidal,[32] R. Vidal,[18] I. Vila,[12] R. Vilar,[12] T. Vine,[31] M. Vogel,[38] I. Volobouev[o],[29] G. Volpi[q],[47] F. Würthwein,[10] P. Wagner,[2] R.G. Wagner,[2] R.L. Wagner,[18] J. Wagner-Kuhr,[27] W. Wagner,[27] T. Wakisaka,[42] R. Wallny,[9] S.M. Wang,[1] A. Warburton,[34] D. Waters,[31] M. Weinberger,[54] W.C. Wester III,[18] B. Whitehouse,[57] D. Whiteson[d],[46] S. Whiteson[k],[17] A.B. Wicklund,[2] E. Wicklund,[18] G. Williams,[34] H.H. Williams,[46] P. Wilson,[18] B.L. Winer,[40] P. Wittich[f],[18] S. Wolbers,[18] C. Wolfe,[14] T. Wright,[35] X. Wu,[21] S.M. Wynne,[30] S. Xie,[33] A. Yagil,[10] K. Yamamoto,[42] J. Yamaoka,[53] U.K. Yang[k],[14] Y.C. Yang,[28] W.M. Yao,[29] G.P. Yeh,[18] J. Yoh,[18] K. Yorita,[14] T. Yoshida,[42] G.B. Yu,[50] I. Yu,[28] S.S. Yu,[18] J.C. Yun,[18] L. Zanello[v],[52] A. Zanetti,[55] I. Zaw,[23] X. Zhang,[25] Y. Zheng[b],[9] and S. Zucchelli[t6]

(CDF Collaboration[‡])

[1]*Institute of Physics, Academia Sinica, Taipei, Taiwan 11529, Republic of China*
[2]*Argonne National Laboratory, Argonne, Illinois 60439*
[3]*University of Athens, 157 71 Athens, Greece*
[4]*Institut de Fisica d'Altes Energies, Universitat Autonoma de Barcelona, E-08193, Bellaterra (Barcelona), Spain*
[5]*Baylor University, Waco, Texas 76798*
[6]*Istituto Nazionale di Fisica Nucleare Bologna,* [t]*University of Bologna, I-40127 Bologna, Italy*
[7]*Brandeis University, Waltham, Massachusetts 02254*
[8]*University of California, Davis, Davis, California 95616*
[9]*University of California, Los Angeles, Los Angeles, California 90024*
[10]*University of California, San Diego, La Jolla, California 92093*
[11]*University of California, Santa Barbara, Santa Barbara, California 93106*
[12]*Instituto de Fisica de Cantabria, CSIC-University of Cantabria, 39005 Santander, Spain*
[13]*Carnegie Mellon University, Pittsburgh, PA 15213*
[14]*Enrico Fermi Institute, University of Chicago, Chicago, Illinois 60637*
[15]*Comenius University, 842 48 Bratislava, Slovakia; Institute of Experimental Physics, 040 01 Kosice, Slovakia*
[16]*Joint Institute for Nuclear Research, RU-141980 Dubna, Russia*
[17]*Duke University, Durham, North Carolina 27708*
[18]*Fermi National Accelerator Laboratory, Batavia, Illinois 60510*
[19]*University of Florida, Gainesville, Florida 32611*
[20]*Laboratori Nazionali di Frascati, Istituto Nazionale di Fisica Nucleare, I-00044 Frascati, Italy*
[21]*University of Geneva, CH-1211 Geneva 4, Switzerland*
[22]*Glasgow University, Glasgow G12 8QQ, United Kingdom*
[23]*Harvard University, Cambridge, Massachusetts 02138*

[24]*Division of High Energy Physics, Department of Physics, University of Helsinki and Helsinki Institute of Physics, FIN-00014, Helsinki, Finland*
[25]*University of Illinois, Urbana, Illinois 61801*
[26]*The Johns Hopkins University, Baltimore, Maryland 21218*
[27]*Institut für Experimentelle Kernphysik, Universität Karlsruhe, 76128 Karlsruhe, Germany*
[28]*Center for High Energy Physics: Kyungpook National University, Daegu 702-701, Korea; Seoul National University, Seoul 151-742, Korea; Sungkyunkwan University, Suwon 440-746, Korea; Korea Institute of Science and Technology Information, Daejeon, 305-806, Korea; Chonnam National University, Gwangju, 500-757, Korea*
[29]*Ernest Orlando Lawrence Berkeley National Laboratory, Berkeley, California 94720*
[30]*University of Liverpool, Liverpool L69 7ZE, United Kingdom*
[31]*University College London, London WC1E 6BT, United Kingdom*
[32]*Centro de Investigaciones Energeticas Medioambientales y Tecnologicas, E-28040 Madrid, Spain*
[33]*Massachusetts Institute of Technology, Cambridge, Massachusetts 02139*
[34]*Institute of Particle Physics: McGill University, Montréal, Canada H3A 2T8; and University of Toronto, Toronto, Canada M5S 1A7*
[35]*University of Michigan, Ann Arbor, Michigan 48109*
[36]*Michigan State University, East Lansing, Michigan 48824*
[37]*Institution for Theoretical and Experimental Physics, ITEP, Moscow 117259, Russia*
[38]*University of New Mexico, Albuquerque, New Mexico 87131*
[39]*Northwestern University, Evanston, Illinois 60208*
[40]*The Ohio State University, Columbus, Ohio 43210*
[41]*Okayama University, Okayama 700-8530, Japan*
[42]*Osaka City University, Osaka 588, Japan*
[43]*University of Oxford, Oxford OX1 3RH, United Kingdom*
[44]*Istituto Nazionale di Fisica Nucleare, Sezione di Padova-Trento,* [u]*University of Padova, I-35131 Padova, Italy*
[45]*LPNHE, Universite Pierre et Marie Curie/IN2P3-CNRS, UMR7585, Paris, F-75252 France*
[46]*University of Pennsylvania, Philadelphia, Pennsylvania 19104*
[47]*Istituto Nazionale di Fisica Nucleare Pisa,* [q]*University of Pisa,* [r]*University of Siena and* [s]*Scuola Normale Superiore, I-56127 Pisa, Italy*
[48]*University of Pittsburgh, Pittsburgh, Pennsylvania 15260*
[49]*Purdue University, West Lafayette, Indiana 47907*
[50]*University of Rochester, Rochester, New York 14627*
[51]*The Rockefeller University, New York, New York 10021*
[52]*Istituto Nazionale di Fisica Nucleare, Sezione di Roma 1,* [v]*Sapienza Università di Roma, I-00185 Roma, Italy*
[53]*Rutgers University, Piscataway, New Jersey 08855*
[54]*Texas A&M University, College Station, Texas 77843*
[55]*Istituto Nazionale di Fisica Nucleare Trieste/ Udine,* [w]*University of Trieste/ Udine, Italy*
[56]*University of Tsukuba, Tsukuba, Ibaraki 305, Japan*
[57]*Tufts University, Medford, Massachusetts 02155*
[58]*Waseda University, Tokyo 169, Japan*
[59]*Wayne State University, Detroit, Michigan 48201*
[60]*University of Wisconsin, Madison, Wisconsin 53706*
[61]*Yale University, New Haven, Connecticut 06520*

We report a measurement of the top quark mass M_t in the dilepton decay channel $t\bar{t} \to b\ell'^{+}\nu'_{\ell}\bar{b}\ell^{-}\overline{\nu}_{\ell}$. Events are selected with a neural network which has been directly optimized for statistical precision in top quark mass using neuroevolution, a technique modeled on biological evolution. The top quark mass is extracted from per-event probability densities that are formed by the convolution of leading order matrix elements and detector resolution functions. The joint probability is the product of the probability densities from 344 candidate events in 2.0 fb^{-1} of $p\bar{p}$ collisions collected with the CDF II detector, yielding a measurement of $M_t = 171.2 \pm 2.7(\text{stat.}) \pm 2.9(\text{syst.})$ GeV/c^2.

PACS numbers: 14.65.Ha, 13.85.Ni, 13.85.Qk, 12.15.Ff

[*]Deceased
[†]Deceased
[‡]With visitors from [a]Universiteit Antwerpen, B-2610 Antwerp, Belgium, [b]Chinese Academy of Sciences, Beijing 100864, China, [c]University of Bristol, Bristol BS8 1TL, United Kingdom, [d]University of California Irvine, Irvine, CA 92697, [e]University of

The most recently discovered charged fermion, the top quark, is the most massive known fundamental particle. Over ten years after the discovery of the top quark, its mass, M_t, remains a quantity of great interest. M_t-dependent terms contribute to radiative corrections to precision electroweak observables, thus helping to constrain contributions by the unobserved Higgs boson [1] and by other particles in possible extensions to the standard model [2]. At present, top quarks can be directly studied only at the Fermilab Tevatron, where they are primarily produced in pairs and decay $\approx 100\%$ to a W boson and a b quark, $t\bar{t} \rightarrow W^+bW^-\bar{b}$, in the standard model. The dilepton channel, where both W bosons decay to charged leptons (electrons and muons, including leptonic decays of τ leptons) and neutrinos, has the smallest branching fraction, but also has the least number of hadronic jets in the final state and hence a smaller sensitivity to their energy calibration. Significant differences in the measurements of M_t in different decay channels could indicate contributions from sources beyond the standard model [3].

Reconstruction of M_t in the dilepton channel presents unique challenges as the presence of the two neutrinos in the final state results in a kinematically underconstrained system. We utilize a likelihood-based estimator that convolutes leading order matrix elements and detector resolution functions and integrates over unmeasured quantities. Prior applications of this method to dilepton events have yielded the most precise measurements of M_t in this channel [4–6]. These prior measurements utilize event selection criteria that were designed to maximize signal purity for a measurement of the $t\bar{t}$ production cross section [7]. Optimization of an event selection is typically hampered by the difficulty of searching the space of arbitrary multivariate selections. Well established multivariate algorithms such as neural networks are typically limited to minimization of a specific metric, such as misclassification error. In contrast with these algorithms, the technique of neuroevolution [8] combines the parametrization of an abitrary multivariate selection described by a neural network with an evolutionary minimization approach to search for the network weights and topology which optimizes an arbitrary metric. In this Letter we present a measurement using an improved matrix element analysis technique and an event selection that uses neuroevolution to optimize for minimal expected statistical uncertainty in the top quark mass measurement. This novel application of neuroevolution yields an event selection with markedly poorer signal purity, yet significantly smaller expected uncertainty in top quark mass. We utilize data collected between March 2002 and May 2007 with the CDF II detector corresponding to an integrated luminosity of 2.0 fb^{-1}.

CDF II [9–11] is a general-purpose detector designed to study $p\bar{p}$ collisions at the Fermilab Tevatron. A charged particle tracking system consisting of a silicon microstrip tracker and a drift chamber is immersed in a 1.4 T magnetic field. Electromagnetic and hadronic calorimeters surround the tracking system and measure particle energies. Drift chambers and scintillators, located outside the calorimeters, detect muons.

The data used in this measurement are collected with lepton triggers that require an electron or muon with $p_T > 18$ GeV/c where the electron $p_T = E_T$ is measured in the calorimeters and the muon p_T is measured in the $|\eta| < 1.2$ region by the tracker. Following this trigger requirement, we define a preselection which satisfies the basic signature of top dilepton decay and provides a starting point for the optimization of selection used in the mass measurement. The pre-selection requires events with two oppositely charged leptons (electrons or muons) with $p_T > 20$ GeV/c, two or more jets with $E_T > 15$ GeV [12] within the region $|\eta| < 2.5$, $\not{E}_T > 20$ GeV [13], and $M_{ll} > 10$ GeV/c^2, where M_{ll} is the invariant mass of the two leptons. Suppression of the $Z \rightarrow ll$ background is left to the neural network selection.

We search for a selection criterion represented by a threshold on the output of an artificial neural network which will yield the most statistically precise measurement of M_t. In high energy physics neural networks are traditionally trained to separate signal and background events in a way that minimizes the mis-classification of signal events as background and vice-versa. This is appropriate for optimizing the sensitivity of counting experiments, but not necessarily for a mass measurement in which some forms of background may be very disruptive and others relatively harmless. The statistical precision is not a trivial function of the signal fraction of the selected sample, because the mass measurement technique includes tools which suppress the effects of some background processes.

We use neuroevolution, an approach modeled on biological evolution, to directly search for the optimal neural network. Beginning with a population of networks with random weights, the statistical precision of M_t is evaluated for each network by performing simulated experi-

---

California Santa Cruz, Santa Cruz, CA 95064, [f]Cornell University, Ithaca, NY 14853, [g]University of Cyprus, Nicosia CY-1678, Cyprus, [h]University College Dublin, Dublin 4, Ireland, [i]University of Edinburgh, Edinburgh EH9 3JZ, United Kingdom, [j]Universidad Iberoamericana, Mexico D.F., Mexico, [k]Informatics Institute, University of Amsterdam, Amsterdam, The Netherlands, [l]University of Manchester, Manchester M13 9PL, England, [m]Nagasaki Institute of Applied Science, Nagasaki, Japan, [n]University de Oviedo, E-33007 Oviedo, Spain, [o]Queen Mary, University of London, London, E1 4NS, England, [p]Texas Tech University, Lubbock, TX 79409, [q]IFIC(CSIC-Universitat de Valencia), 46071 Valencia, Spain, [x]Royal Society of Edinburgh/Scottish Executive Support Research Fellow, [y]Istituto Nazionale di Fisica Nucleare, Sezione di Cagliari, 09042 Monserrato (Cagliari), Italy

TABLE I: Expected sample composition after neural network selection for events with and without secondary vertex tags. The prediction for $t\bar{t}$ is shown for a production cross-section of 6.7 pb and $M_t = 175$ GeV/c^2.

Source	N(0-tag)	$N(\geq$ 1-tag)
$Z \to ll$	116.5 ± 18.6	4.1 ± 1.8
$Z \to ll + c\bar{c}/b\bar{b}$	9.3 ± 1.4	10.1 ± 4.0
$WW, WZ, ZZ, W\gamma$	17.3 ± 5.9	0.7 ± 0.7
Misidentified leptons	29.0 ± 8.7	4.5 ± 1.1
$t\bar{t}$ ($\sigma = 6.7$ pb)	43.8 ± 4.4	78.0 ± 6.2
Total	215.8 ± 21.9	97.5 ± 7.2
Observed (2.0 fb^{-1})	246	98

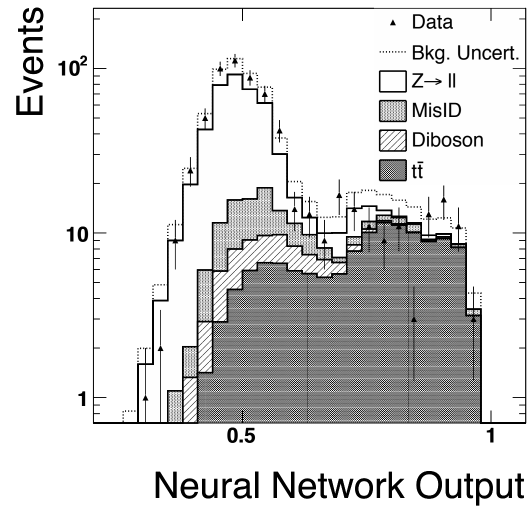

FIG. 1: The output of the final network evaluated on the collected data (black triangles), with expected signal and background contributions (stacked solid histograms). The data show events passing the pre-selection. The evolution of the optimum selection network is performed with an *a priori* threshold set at 0.5 for candidate selection. Of the 642 pre-selected events shown, 344 events pass this threshold and constitute the final candidate sample for mass-fitting.

ments using the simulated signal and background events for which the network output is greater than 0.5. The events used are generated using the PYTHIA [14] and ALPGEN [15] generators and are evaluated with a full detector simulation [16]. Poor performers are culled and strong performers are bred together and mutated in successive generations until performance reaches a plateau. Because we have optimized directly on the final statistical precision rather than some intermediate or approximate figure of merit, the best-performing network is the one which gives the most precise measurement. This approach has been shown to significantly outperform traditional methods in event selection [17]. In particular, we use neuroevolution of augmenting topologies (NEAT) [18], a neuroevolutionary method capable of evolving a network's topology in addition to its weights.

We separate events passing this selection into events with and events without displaced tracks, or secondary vertex tags [19], which enhance b-quark fraction and thus signal purity. The predicted number of signal events and background events with real or misidentified ("fake") leptons in 2.0 fb^{-1} is shown in Table I for events with and without secondary vertex tags. Using the optimized selection improves the *a priori* statistical uncertainty on M_t over the selection used in previous versions [6] of this analysis by 20%. This neural network selection yields 344 candidate events in the sample reported in this Letter as illustrated in Fig. 1. Strikingly, the sample selected by the neural network is expected to be dominated by background events; the resulting measurement is expected to be more precise than previous measurements due to the increase in $t\bar{t}$ acceptance and the suppression of problematic background effects as described below.

We express the probability density for the vector of observed lepton and jet energy measurements, $\mathbf{x}_i$, as a function of the top quark mass M_t as $P_s(\mathbf{x}_i|M_t)$. We calculate $P_s(\mathbf{x}_i|M_t)$ using the theoretical description of the $t\bar{t}$ production and decay process with respect to $\mathbf{x}_i$, $P_s(\mathbf{x}_i|M_t) = [1/\sigma(M_t)][d\sigma(M_t)/d\mathbf{x}_i]$, where $\frac{d\sigma}{d\mathbf{x}_i}$ is the differential cross section and σ is the total cross section.

We evaluate $P_s(\mathbf{x}_i|M_t)$ by integrating over quantities that are not directly measured by the detector, such as neutrino momenta and quark energies. We assume that lepton energies and quark angles are perfectly measured, that incoming partons are massless and have no transverse momentum, and that the two most energetic jets in the event correspond to the b quarks (with a mass of 4.7 GeV/c^2) from $t\bar{t}$ decay. The effect of these assumptions on the final measurement is estimated using simulated experiments. While quark energies cannot be directly measured, they can be estimated from measured jet energies. We integrate over quark energies using a parameterized transfer function [5] that describes detector effects. This transfer function $W(p, j)$ is defined to be the probability of measuring jet energy j, given quark energy p. The expression for the probability density at a given mass for a specific event can be written as

$$P_s(\mathbf{x}_i|M_t) = \frac{1}{\sigma(M_t)} \int d\Phi |\mathcal{M}_{t\bar{t}}(q_k, p_k; M_t)|^2 \times \quad (1)$$
$$f_{PDF}(q_1) f_{PDF}(q_2) \prod_{jets} W(p_k, j_k),$$

where the integral $\int d\Phi$ is over the momenta of the initial and final state particles, q_1 and q_2 are the incoming parton momenta, p_k are the outgoing momenta, $f_{PDF}(q_k)$ are the parton distribution functions (PDFs) [20], and $\mathcal{M}_{t\bar{t}}(q_k, p_k; M_t)$ is the leading-order $t\bar{t}$ production and decay matrix element as defined in [21, 22] for the process $q\bar{q} \rightarrow t\bar{t} \rightarrow b\ell^+\nu_\ell \bar{b}\ell'^-\bar{\nu}_{\ell'}$ [23]. The term $1/\sigma(M_t)$ ensures that the probability density satisfies the normalization condition, $\int d\mathbf{x}_i\ P_s(\mathbf{x}_i|M_t) = 1$.

The probability $P_s(\mathbf{x}_i|M_t)$ is sufficient to extract the top quark mass in a pure $t\bar{t}$ sample. However, the event selection we use maximizes signal acceptance at the expense of accepting a significant number of background events. To reduce the effect of background on the measurement, we calculate the probability densities $P_{bg_k}(\mathbf{x}_i)$ of observing an event $\mathbf{x}_i$ given a background process. We form the full per-event probability as

$$P^{n-tag}(\mathbf{x}_i|M_t) = P_s(\mathbf{x}_i|M_t)p_s^{n-tag} + \sum_k P_{bg_k}(\mathbf{x}_i)p_{bg_k}^{n-tag}, \tag{2}$$

which is a sum of the probability densities for each process, weighted by their respective *a priori* proportions. The functions $P_{bg_k}(\mathbf{x}_i)$ are formed by calculating a differential cross-section for each background process in a manner similar to $t\bar{t}$. The proportions for each process, p_s^{n-tag} and $p_{bg_k}^{n-tag}$ depend on whether the event has a secondary vertex tag, and are fixed to the expected fractions of signal and background events in each category, listed in Table I.

The background processes for which we evaluate probability densities are: $Z/\gamma^* \rightarrow ee, \mu\mu$ plus associated jets, W plus three or more associated jets where one jet is incorrectly identified as a lepton, and WW plus associated jets. probability densities for smaller backgrounds (WZ, ZZ, $W\gamma$, and $Z \rightarrow \tau\tau$) provide negligible gain in sensitivity and are not modeled.

The posterior joint probability for the sample is the product of the per-event probability densities,

$$P(\mathbf{x}|M_t) = \Big[\prod_{i_0} P^{0-tag}(\mathbf{x}_{i_0}|M_t)\Big] \times \Big[\prod_{i_1} P^{\geq 1-tag}(\mathbf{x}_{i_1}|M_t)\Big], \tag{3}$$

where the products are over all untagged events i_0 and all tagged events i_1. The measured mass M_t is taken as the mean of the posterior probability, and the measured statistical uncertainty ΔM_t is taken as the standard deviation.

The response of our method for simulated experiments is shown in Fig. 2a. While the response is consistent with a linear dependence on the true top mass, its slope is less than unity due to the presence of unmodeled background in our sample. We derive corrections, $M_t \rightarrow 171.0\ \mathrm{GeV}/c^2 + (M_t - 175.0\ \mathrm{GeV}/c^2)/0.86$ and $\Delta M_t \rightarrow \Delta M_t/0.86$, from this response and apply them to the measured quantities in data.

From the pull distribution of our simulated experiments, we find that the statistical uncertainty is underestimated, as shown in Fig. 2b. This is due to simplifying assumptions made in the probability calculations in the interest of computational tractability [5]. These assumptions are violated in small, well-understood ways in realistic events. To account for this underestimation, we scale the statistical uncertainty by an additional factor, $S = 1.16$, derived from the results of our simulated experiments. Correcting by this factor, we estimate the expected statistical uncertainty to be 2.7 GeV/c^2 if $M_t = 175$ GeV/c^2.

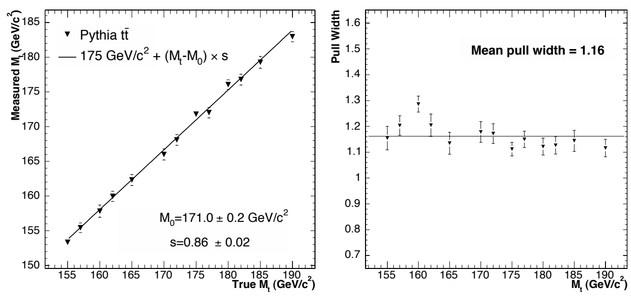

(a) (b)

FIG. 2: *(a)* Mean measured M_t in simulated experiments versus top quark masses. The solid line is a linear fit to the points. *(b)* Pull widths from simulated experiments versus top quark masses. The solid line is the average over all points.

Applying the method and corrections described above to the 344 candidate events passing our selection, we measure $M_t = 171.2 \pm 2.7(\mathrm{stat.})$ GeV/c^2. The negative of the logarithm of the joint probability density for all 344 events is shown in Fig. 3.

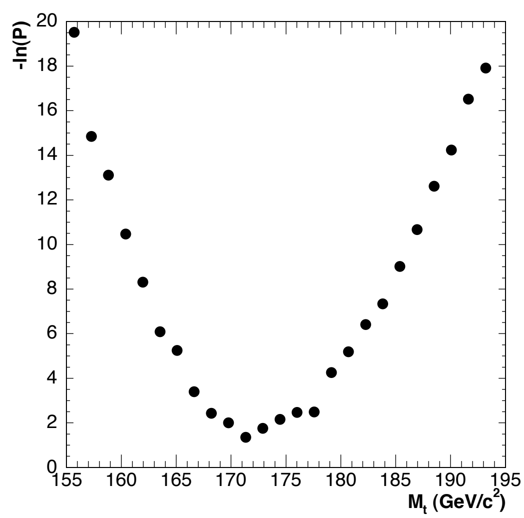

FIG. 3: Negative of the logarithm of the joint probability density as a function of top quark mass for the 344 candidate events after all corrections. Systematic uncertainties are not shown.

There are several sources of systematic uncertainty in our measurement, which are summarized in Table II. The single largest source of systematic error comes from the uncertainty in the jet energy scale, which we estimate to be 2.5 GeV/c^2 by varying the scale within its uncertainty [24]. An uncertainty specific to jets result-

TABLE II: Summary of systematic uncertainties on the measured top quark mass.

Source	Size (GeV/c^2)
Generic jet energy scale	2.5
b-Jet Energy Scale	0.4
In-time pileup	0.2
Generator	0.9
PDFs	0.6
Background statistics	0.5
Radiation	0.5
Response correction	0.4
Sample composition uncertainty	0.3
Background modeling	0.2
Lepton energy scale	0.1
Total	2.9

ing from b partons contributes 0.4 GeV/c^2 while in-time pileup contributes 0.2 GeV/c^2. Uncertainty due to the Monte Carlo generator used for $t\bar{t}$ events is estimated as the difference in the extracted top quark mass from PYTHIA events and HERWIG [25] events and amounts to 0.9 GeV/c^2. Uncertainties due to PDFs are estimated using different PDF sets (CTEQ5L [20] vs. MRST72 [26]) and values of Λ_{QCD} and varying the eigenvectors of the CTEQ6M [20] set; the quadrature sum of these uncertainties is 0.6 GeV/c^2. The limited number of background events available for simulated experiments results in an uncertainty on the shape of the background distributions, which yields an uncertainty on M_t of 0.5 GeV/c^2. Uncertainty due to imperfect modeling of initial and final state QCD radiation (ISR and FSR, respectively) is estimated by varying the amounts of ISR and FSR in simulated events [27] and is estimated to be 0.5 GeV/c^2. The uncertainty in the mass due to uncertainties in the response correction is evaluated by varying the response within the uncertainties shown in Fig. 2a and is 0.4 GeV/c^2. The contribution from uncertainties in background composition is estimated by varying the background normalizations from Table I within their uncertainties and amounts to 0.3 GeV/c^2. We estimate the uncertainty coming from modeling of the missing tranverse energy in Z/γ^* events and the uncertainty in the data-derived model of misindentified leptons to be 0.2 GeV/c^2. The uncertainty in the lepton energy scale contributes an uncertainty of 0.1 GeV/c^2 to our measurement. Adding all of these contributions together in quadrature yields a total systematic uncertainty of 2.9 GeV/c^2.

In summary, we have presented a new measurement of the top quark mass in the dilepton channel. We have applied the technique of neuroevolution, for the first time in particle physics, to devise an event selection criterion which optimizes the statistical precision of this measurement. We measure $M_t = 171.2 \pm 2.7(\text{stat.}) \pm 2.9(\text{syst.})$ GeV/c^2. This is the single most precise measurement of M_t in this channel to date, is in good agreement with measurements in other channels [28, 29], and represents a ∼30% improvement in statistical precision over the previously published measurements in this channel [6, 30, 31].

We thank the Fermilab staff and the technical staffs of the participating institutions for their vital contributions. This work was supported by the U.S. Department of Energy and National Science Foundation; the Italian Istituto Nazionale di Fisica Nucleare; the Ministry of Education, Culture, Sports, Science and Technology of Japan; the Natural Sciences and Engineering Research Council of Canada; the National Science Council of the Republic of China; the Swiss National Science Foundation; the A.P. Sloan Foundation; the Bundesministerium für Bildung und Forschung, Germany; the Korean Science and Engineering Foundation and the Korean Research Foundation; the Science and Technology Facilities Council and the Royal Society, UK; the Institut National de Physique Nucleaire et Physique des Particules/CNRS; the Russian Foundation for Basic Research; the Ministerio de Educación y Ciencia and Programa Consolider-Ingenio 2010, Spain; the Slovak R&D Agency; and the Academy of Finland.

[1] The LEP Collaboration, The LEP Electroweak Working group, The SLD Electroweak and Heavy Flavor Groups (LEP), Tech. Rep. CERN-PH-EP/2007-039, CERN (2007).
[2] S. Heinemeyer *et al.*, J. High Energy Phys. **0309**, 075 (2003).
[3] G. L. Kane and S. Mrenna, Phys. Rev. Lett. **77**, 3502 (1996).
[4] A. Abulencia *et al.* (CDF Collaboration), Phys. Rev. Lett. **96**, 152002 (2006).
[5] A. Abulencia *et al.* (CDF Collaboration), Phys. Rev. D **74**, 032009 (2006).
[6] A. Abulencia *et al.* (CDF Collaboration), Phys. Rev. D **75**, 031105 (2007).
[7] D. Acosta *et al.* (CDF Collaboration), Phys. Rev. Lett. **93**, 142001 (2004).
[8] X. Yao, Proceedings of the IEEE **87**, 1423 (1999).
[9] D. Acosta *et al.* (CDF Collaboration), Phys. Rev. D **71**, 032001 (2005).
[10] A. Abulencia *et al.* (CDF Collaboration), J. Phys. G **34**, 2457 (2007).
[11] CDF uses a cylindrical coordinate system with the z axis along the proton beam axis. Pseudorapidity is $\eta \equiv -\ln(\tan\theta/2)$, where θ is the polar angle, and ϕ is the azimuthal angle relative to the proton beam direction, while $p_T = |p| \sin\theta$, $E_T = E \sin\theta$.
[12] F. Abe *et al.* (CDF Collaboration), Phys. Rev. D **45**, 1448 (1992).
[13] Missing transverse energy, $\not{E}_T$, is defined as the magnitude of the vector $-\sum_i E_T^i \vec{n}_i$ where E_T^i are the magnitudes of transverse energy contained in each calorimeter tower i, and $\vec{n}_i$ is the unit vector from the interaction vertex to the tower in the transverse (x, y) plane.

[14] T. Sjostrand *et al.*, Computer Phys. Commun. **135**, 238 (2001).
[15] M. L. Mangano *et al.*, J. High Energy Phys. **0307**, 001 (2003).
[16] T. Affolder *et al.*, Nucl. Instrum. Methods A **447**, 1 (2000).
[17] S. Whiteson and D. Whiteson, in *Proceedings of the Twenty-Second AAAI Conference on Artificial Intelligence, July 22-26, 2007, Vancouver, British Columbia, Canada* (AAAI Press, 2007), ISBN 978-1-57735-323-2.
[18] K. O. Stanley and R. Miikkulainen, Evolutionary Computation **10(2)**, 99 (2002).
[19] D. Acosta *et al.* (CDF Collaboration), Phys. Rev. **71**, 052003 (2005).
[20] J. Pumplin *et al.*, J. High Energy Phys. **012**, 0207 (2002).
[21] G. Mahlon and S. Parke, Phys. Lett. B **411**, 173 (1997).
[22] G. Mahlon and S. Parke, Phys. Rev. D **55**, 7249 (1997).
[23] While up to 15% of $t\bar{t}$ pairs at the Tevatron are produced by gluon-gluon fusion ($gg \to t\bar{t}$), this term can be excluded from the matrix element with negligible effect on the measurement.
[24] A. Bhatti *et al.*, Nucl. Instrum. Methods A **566**, 375 (2006).
[25] G. Corcella *et al.*, J. High Energy Phys. **01**, 010 (2001).
[26] A. D. Martin *et al.*, Phys. Lett. B **356**, 89 (1995).
[27] A. Abulencia *et al.* (CDF Collaboration), Phys. Rev. D **73**, 32003 (2006).
[28] T. Aaltonen *et al.* (CDF Collaboration), Phys. Rev. Lett. **99**, 182002 (2007).
[29] T. Aaltonen *et al.* (CDF Collaboration), Phys. Rev. D **76**, 072009 (2007).
[30] T. Aaltonen *et al.* (CDF Collaboration), Phys. Rev. Lett. **100**, 062005 (2008).
[31] V. Abazov *et al.* (DØ Collaboration), Phys. Lett B **655**, 7 (2007).